Divergence-Free Transport of Laser-Produced Fast Electrons Along a Meter-Long Wire Target

Hiroaki Nakajima, Shigeki Tokita,* Shunsuke Inoue, Masaki Hashida, and Shuji Sakabe

Institute for Chemical Research, Kyoto University, Gokasho, Uji, Kyoto 611-0011, Japan and Department of Physics, Graduate School of Science, Kyoto University, Kitashirakawa, Sakyo, Kyoto 606-7501, Japan

(Received 14 December 2012; published 8 April 2013)

We demonstrate that, from a 10-μm metal wire irradiated by a 10^{19} W/cm^2 laser pulse, fast electrons form a nearly perfect circular beam around the wire and propagate along it. The total charge and diameter of the electron beam are maintained over a propagation distance of 1 m. Moreover, the electron beam can be guided along a slightly bent wire. Numerical simulations suggest that a relatively weak steady electric field, which does not decay for several nanoseconds, is generated around the wire and plays a key role in the long-distance guidance.

DOI: 10.1103/PhysRevLett.110.155001 PACS numbers: 52.38.Kd, 41.75.Jv, 52.50.Jm

The development of ultraintense lasers [1] has facilitated the generation of high-current charged particle beams [2–4]; however, the control of such beams (collimation, transport, and focusing) remains a challenge [5–15]. Collimation and guidance of fast electrons by using a wire plasma has been demonstrated over a 1-mm distance [9]. This effect is attributed to the balance between the electric and magnetic forces acting on the relativistic electrons (moving near the speed of light) in the vicinity of the wire surface. A strong electric field of the order of 10^{12} V/m affects the electrons in this case. Such a fast electron phenomenon has been observed at the surface of a planar target [5–8]. Collimation of fast electrons using a wire with a length of the order of centimeters has also been demonstrated [12]. In this case, the effect is attributed to a transient balance between the electric force and the centrifugal force. The balanced force is estimated to be relatively weak, corresponding to an electric field of the order of 10^8 V/m. This collimation mechanism could be used for long-distance guidance of electrons. However, the strong field produced on the wire surface cannot exist for a long time because it originates from the space charge of an expanding fast electron bunch emitted into vacuum from the laser irradiated spot. Here we report the observation that a metal wire can act as a guiding device for an electron beam. We have observed that a significant number of fast electrons can be guided over 1 m along a metal wire, without a change in beam size. The experimental results for the transverse distribution of the electron beam are well reproduced by numerical simulations of electron trajectories based on a simplified model.

The experiments were performed with a terawatt 150-fs Ti:sapphire laser system. A laser pulse with a pulse energy of 250 mJ was focused to a spot size 3 μm $\times$ 4 μm with an off-axis parabolic mirror, resulting in a peak intensity of $\sim 10^{19}$ W/cm^2. The contrast ratio of the intensity of the main pulse to that of the amplified spontaneous emission was 10^7. The laser beam with p polarization was irradiated onto a tungsten wire with a diameter of 10 μm at an incidence angle of 45°. The experiments were performed in a vacuum chamber with a pressure of 0.02 Pa.

First, we simply measured the spatial distribution of the electrons emitted from the metal wire by using triple-layer stacked imaging plates (IPs) at the end of a wire tightened using a small weight [see Fig. 1(a)]. The IPs have high sensitivity for electrons in the energy range from 40 to 1000 keV and are most sensitive at around 200 keV [16]. On the second and the third layer of the stacked IPs, electrons with energies higher than $\sim$400 and $\sim$600 keV can be detected, respectively. Each IP had a pinhole with a 1-mm diameter to allow the wire to pass through. Figure 2 shows typical single-shot images at $L = 150$, 400, and 1050 mm, where L is the distance from the laser irradiated spot to the end of the wire. The black spots in the center are the nondetecting areas formed by the pinhole in each IP. On the first layer IP, the signal is saturated near the center to a maximum electron density of the order of 4×10^{-9} C/cm^2. The full width at half-maximum (FWHM) of the central part of the images on the second layer IP is 3 to 4 mm, and the images on the third layer IP are similar to those on the second layer. Thus, the distribution of high energy electrons (higher than about 400 keV) did not depend significantly on the electron energy. The beam patterns for each wire length were highly reproducible; however, the beam size showed slight shot-to-shot fluctuation of less than ± 1 mm. Assuming a typical electron energy to be 100 keV, the total charge of detected electrons was estimated to be at least 3 nC by integrating the signals below the saturation level. It was also found that the total charge does not depend significantly on the wire length L.

If the electrons do not interact with the wire, the electron beam ought to escape from the end of the wire with no change of transverse momentum. In the next step, we measured the spatial distribution of the electrons beyond the end of the wire [Fig. 1(b)]. The end of the wire was supported in two directions by two polyamide fibers of 15 μm in diameter, which were connected to the metal wire using an adhesive. The distance from the laser focal

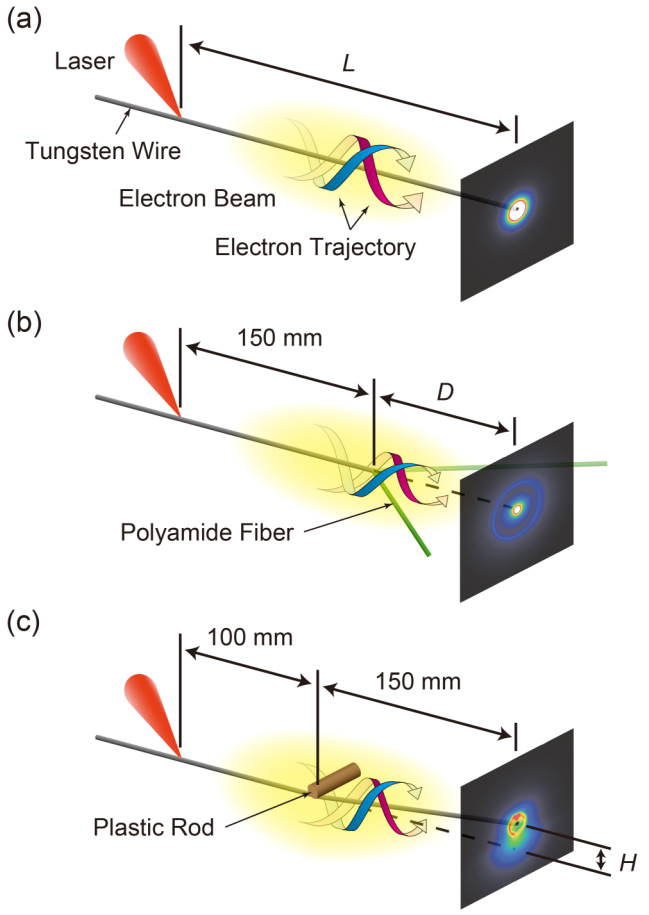

FIG. 1 (color online). The experimental setups used to observe the spatial distributions of electrons generated from a metal wire. (a) The end of the wire, (b) beyond the end of the wire, and (c) at the end of a wire bent in the middle.

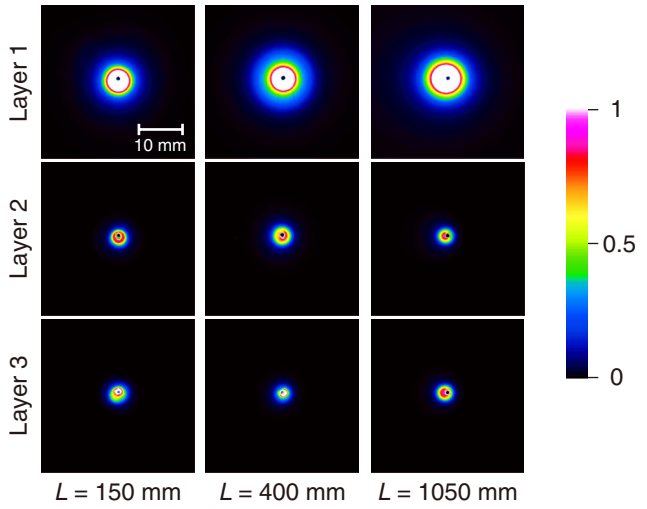

FIG. 2 (color online). Typical single-shot images at $L = 150$, 400, and 1050 mm generated from the setup in Fig. 1(a). The actual size of the images is 35 mm × 35 mm. In each image, the maximum value is normalized to unity. The central black spots are nondetecting areas formed by the pinhole made to allow the wire to pass through the imaging plates.

spot to the end of the wire was 150 mm. Figure 3(a) shows the typical spatial distributions at $D = 50$ and 100 mm, where D is the distance from the wire end to the detection plane. Each image shows a center spot and a coaxial ring that is significantly different from that in the preceding experiment. The diameters of the center spot at $D = 50$ mm were 1.3 and 1.4 mm at FWHM on the second and third layer IPs, respectively. These diameters are smaller than those measured at the end of the wire in the previous experiment. However, the spot diameter at the second layer increased by about 40% after only 50 mm of free-space propagation, resulting in a beam divergence of 1.6 mrad. The diameter of the coaxial ring also increased from 14 to 28 mm with the propagation from $D = 50$ to 100 mm; consequently, the diameter of the ring was estimated to be approximately zero at the end of the wire. The total charge included in the center spot was estimated to be 0.8 nC at $D = 100$ mm. This charge corresponds to less than 30% of that measured at the end of the wire. It, therefore, appears that a significant number of electrons were scattered at the end of the wire. This indicates that the interaction between the wire and the electron beam was large enough to affect the divergence of the electron beam. We also used a magnetic energy analyzer to measure the energy spectrum of the electrons at $D = 30$ mm. The energy spectrum has a peak around 50 to 100 keV and most of the emitted electrons have energies lower than 500 keV [Fig. 3(b)].

To confirm that a metal wire can act as a flexible guiding device, we measured the spatial distribution of the electrons for a wire that was slightly bent in the middle [Fig. 1(c)]. The wire was bent by a plastic rod with a diameter of 20 mm at a distance of 100 mm from the focal spot. The difference in height between the wire end and the laser focal spot is denoted by H. Figure 4 shows typical single-shot images for $H = 5$ and 20 mm. These imaging plates are not saturated. At $H = 5$ mm, most of electrons are distributed around the position of the wire end and lie above the position of the original wire axis, showing that the electron beam was guided along the wire. Moreover, although half of the electrons were lost due to blocking by the plastic rod when the beam passed through the bending point, the electron beam produced a ring-shaped profile at the IP; this shows that the electrons had an azimuthal velocity around the wire. In contrast, for $H = 20$ mm, the electrons were distributed around the position of the original wire axis, showing that the electron beam escaped from the wire at a large bending angle. From these results we can roughly estimate the attractive force between the electrons and the wire. If a wire is bent at a point with an angle of θ, an electron propagating parallel and near to the wire is released from the wire with a radial velocity $v_r = v \sin\theta$. If the electron has a radial kinetic energy larger than the potential energy of the attractive force, the electron can

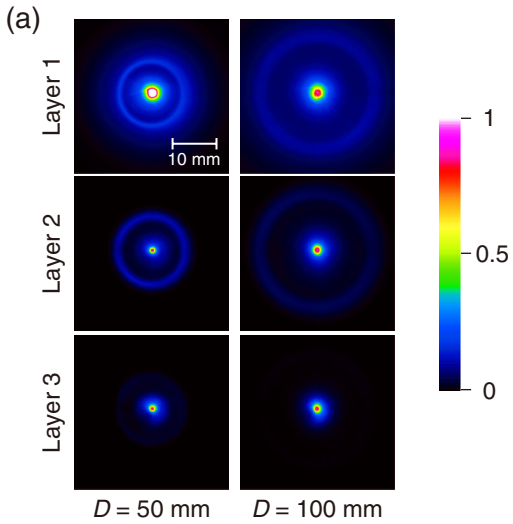

FIG. 3 (color online). (a) Typical single-shot images at $D = 50$ and 100 mm using the setup in Fig. 1(b). The actual size of the images is 35 mm × 35 mm. In each image, the maximum value is normalized to unity. (b) The energy spectrum of the electrons at $D = 30$ mm.

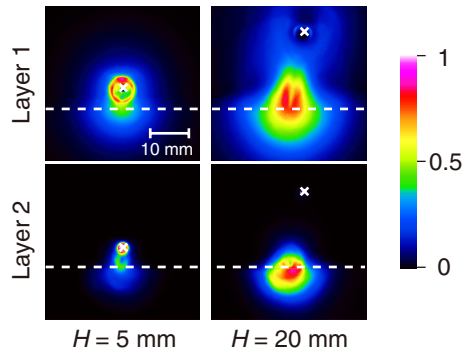

FIG. 4 (color online). Typical single-shot images at $H = 5$ and 20 mm using the setup in Fig. 1(c). The actual size of the images is 40 mm × 40 mm. In each image, the maximum value is normalized to unity. The dotted line and the cross show the height of the focal spot and the wire end, respectively.

escape from the wire. Assuming a static electric field surrounding a positive-charged wire and an electron energy of 100 keV, the electric field can be estimated to be larger than $\sim 10^6$ V/m at the wire surface.

Our experimental results suggest that the electron beam was bound by a steady field surrounding the wire over a period of several nanoseconds. From previous studies [9,12], the collimation and short-distance guidance of fast electrons with a metal thin wire irradiated by an intense laser pulse are thought to be caused by the balance of the attractive electric force, the repulsive magnetic force, and the repulsive centrifugal force, where the electric field is produced by the space charge of the fast electrons emitted from the laser irradiated spot. In general, such an electric field rapidly decreases with a time constant of a picosecond to tens of picoseconds due to the natural expansion of the fast electron bunch. In the present experiment, the collimation and the guidance in the early stage immediately after a laser irradiation can be explained as the effects of a rapidly decreasing electric field. However, to explain the long-distance guidance, we need to introduce an additional electric field that is maintained over a long period of time.

To simulate the experimental result, we simplified a model that approximately simulates the electric field on the metal wire [12]. We assume that the strength of the radial electric field at a radial distance r from the axis can be approximated by $1/r$ outside the wire, and the electric field at time t after the laser irradiation can be expressed as a uniform line charge that decays with time: the line charge density is given by $\rho(t) = \rho_1 \exp(-t/\tau_1) + \rho_2 \exp(-t/\tau_2) + \rho_3$. The axial electric field and the magnetic field are ignored. Although the electric field around the wire is in fact not uniform and not electrostatic, this assumption gives a good approximation that the electrons are subjected to electric forces around the wire from the sheath electric field. All electrons are emitted from the circumference of the wire. The initial energy distribution of the electrons is uniform in the range of 50–1000 keV, and the angular distribution is uniform in all directions. The electrons injected into the wire area are excluded. The results of the simulation are shown as the spatial distributions of electrons passing through screens at 150, 400, and 1050 mm from the electron source [Fig. 5(a)] and as typical electron trajectories [Fig. 5(b)]. To reproduce the experimental results, the parameters ρ_1, ρ_2, ρ_3, τ_1, and τ_2 are set to 8000, 1000, 1.5 nC/m, and 2 and 65 ps, respectively, resulting in an initial electric field of 3×10^{10} V/m at the wire surface. For these conditions, although the electrons are emitted in random directions, a significant fraction of electrons (several percent of the number of the initial electrons) are collimated by the initial strong electric field. The collimated electrons are strongly attracted to the wire more than 50 mm from the electron source because of the electric field, which decays within several hundreds of picoseconds. After that, the electrons are weakly attracted because of the steady electric field (5×10^6 V/m at the surface, originating from ρ_3). For higher steady electric

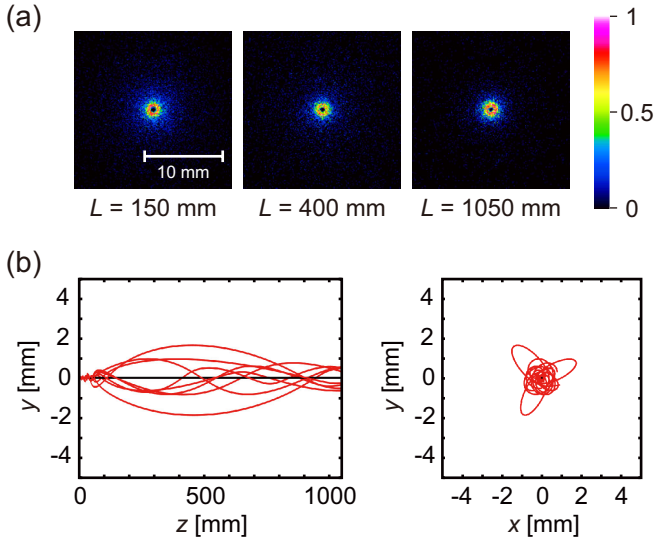

FIG. 5 (color online). (a) Simulation results of spatial distributions at 150, 400, and 1050 mm from the electron source. The actual size of the images is 20 mm × 20 mm. (b) Fifteen electron trajectories are in the simulation.

field (higher ρ_3), the electron trajectories show similar behavior but the electron distribution tends to concentrate around the wire. In contrast, without the steady electric field ($\rho_3 = 0$), the electrons spread out after the early-stage attraction. Therefore, the simulation result suggests that the relatively weak electric field maintained during the electron propagation over 1 m plays a key role in the long-distance guidance. Moreover, the weak electric field assumed in the simulation is roughly comparable to the one estimated from the experimental results for the bent wire. Physically, such a long-lived electric field can be generated on the metal wire by a static electric charge or by a surface electromagnetic wave [17].

We have demonstrated that a metal wire works as a guiding device, analogous to an optical fiber, for a broad-energy electron beam with a charge of more than a few nanocoulombs and sub-megaelectronvolt energy. Such a device could enable the efficient transportation of energy from an intense broad-energy electron source, such as a relativistic laser plasma. Although now the energy conversion efficiency from laser to electron beam is merely of the order of 0.1% and the kinetic energy of the guided electron beam is at the 100 keV level, we believe that we will be able to improve these parameters in future studies. For example, increasing the laser power should bring about improvements, because a laser pulse with a higher intensity will produce more high-energy electrons with a greater conversion efficiency, as well as a stronger field on the wire.

This work was supported by JSPS KAKENHI Grants No. 22654050, No. 24540537, and No. 23226002. Partial support was also provided by The Mitsubishi Foundation, the Yamada Science Foundation, and a Grant-in-Aid for the Global COE Program from the Ministry of Education, Culture, Sports, Science and Technology (MEXT), Japan. H. N. and S. T. contributed equally to this work.

*Corresponding author.
tokita@laser.kuicr.kyoto-u.ac.jp

[1] M. D. Perry and G. Mourou, Science **264**, 917 (1994).
[2] H. M. Key *et al.*, Phys. Plasmas **5**, 1966 (1998).
[3] R. Kodama *et al.*, Nature (London) **412**, 798 (2001).
[4] R. A. Snavely *et al.*, Phys. Rev. Lett. **85**, 2945 (2000).
[5] Y. T. Li *et al.*, Phys. Rev. Lett. **96**, 165003 (2006).
[6] X. H. Yuan *et al.*, Phys. Plasmas **15**, 013106 (2008).
[7] Z. Li *et al.*, Phys. Plasmas **13**, 043104 (2006).
[8] J. Y. Mao *et al.*, Phys. Rev. E **85**, 025401 (2012).
[9] R. Kodama *et al.*, Nature (London) **432**, 1005 (2004).
[10] J. S. Green *et al.*, Nat. Phys. **3**, 853 (2007).
[11] J. Pasley *et al.*, Phys. Plasmas **14**, 120701 (2007).
[12] S. Tokita, K. Otani, T. Nishoji, S. Inoue, M. Hashida, and S. Sakabe, Phys. Rev. Lett. **106**, 255001 (2011).
[13] T. Toncian *et al.*, Science **312**, 410 (2006).
[14] S. Kar *et al.*, Phys. Rev. Lett. **100**, 105004 (2008).
[15] T. Bartal *et al.*, Nat. Phys. **8**, 139 (2011).
[16] A. Taniyama, D. Shindo, and T. Oikawa, J. Electron Microsc. **46**, 303 (1997).
[17] G. Goubau, J. Appl. Phys. **21**, 1119 (1950).